Electronic Supplementary Material (ESI) for Chemical Communications

SUPPORTING INFORMATION

Short, terminally modified 2'-OMe RNAs as inhibitors of microRNA

Jenny Blechinger,[a] Hanna Pieper,[a] Paul Marzenell,[a] Larisa Kovbasyuk,[a] Andrius Serva, [b,c] Vytaute Starkuviene,[b] Holger Erfle,[b] Andriy Mokhir*[a]

[a] Organic Chemistry II, Friedrich-Alexander -University of Erlangen, Henkestr. 42, 91054 Erlangen, Germany
[b] BioQuant, Ruprecht-Karls-University of Heidelberg, Im Neuenheimer Feld 267, Heidelberg, Germany
[c] current address: Division of Molecular Genetics, German Cancer Research Center (DKFZ),Im Neuenheimer Feld 580, 69120 Heidelberg, Germany

Commercially available chemicals of the best quality from Aldrich/Sigma/Fluka (Germany) were obtained and used without purification. Phosphoramidites and controlled pore glass (CPG) solid support were from Glen Research (USA) and Link Technologies (UK). MALDI-TOF mass spectra were recorded on a Bruker Microflex mass spectrometer. The matrix mixture (2:1, v/v) was prepared from 2′,4′,6′-trihydroxyacetophenone (THAP, 0.3 M solution in acetonitrile) and diammonium citrate (0.1 M in water). Samples for the mass spectrometry were prepared by the dried-droplet method by using a 1:2 probe/matrix ratio. Mass accuracy with external calibration was 0.1% of the peak mass, that is, $\pm$ 7.0 at m/z 7000. HPLC was performed at 22 °C on a Shimadzu liquid chromatograph equipped with a UV detector and a Macherey–Nagel Nucleosil C4 250 x 4.6 mm column using gradients of solution B (CH_3CN)) in solution A (0.1 M (NEt_3H)(OAc)). UV/Vis spectra were measured on a Lambda Bio+ UV/Vis spectrophotometer (Perkin Elmer) by using microcuvettes with a sample volume of 70 µL. Fluorescence spectra were acquired on a Varian Cary Eclipse fluorescence spectrophotometer by using black-wall fluorescence semimicrocuvettes (Hellma GmbH, Germany) with a sample volume of 0.7 mL. Chemiluminescence measurements were conducted on a plate reader Mithras LB940 (Berthold Technologies).

Screening of terminal modifications on 14-mer inhibitors of miR-92

Structures and labeling scheme of inhibitors are summarized in Scheme S1 and Table S1. Characterization data as well as inhibitor properties are provided below (Table S2).

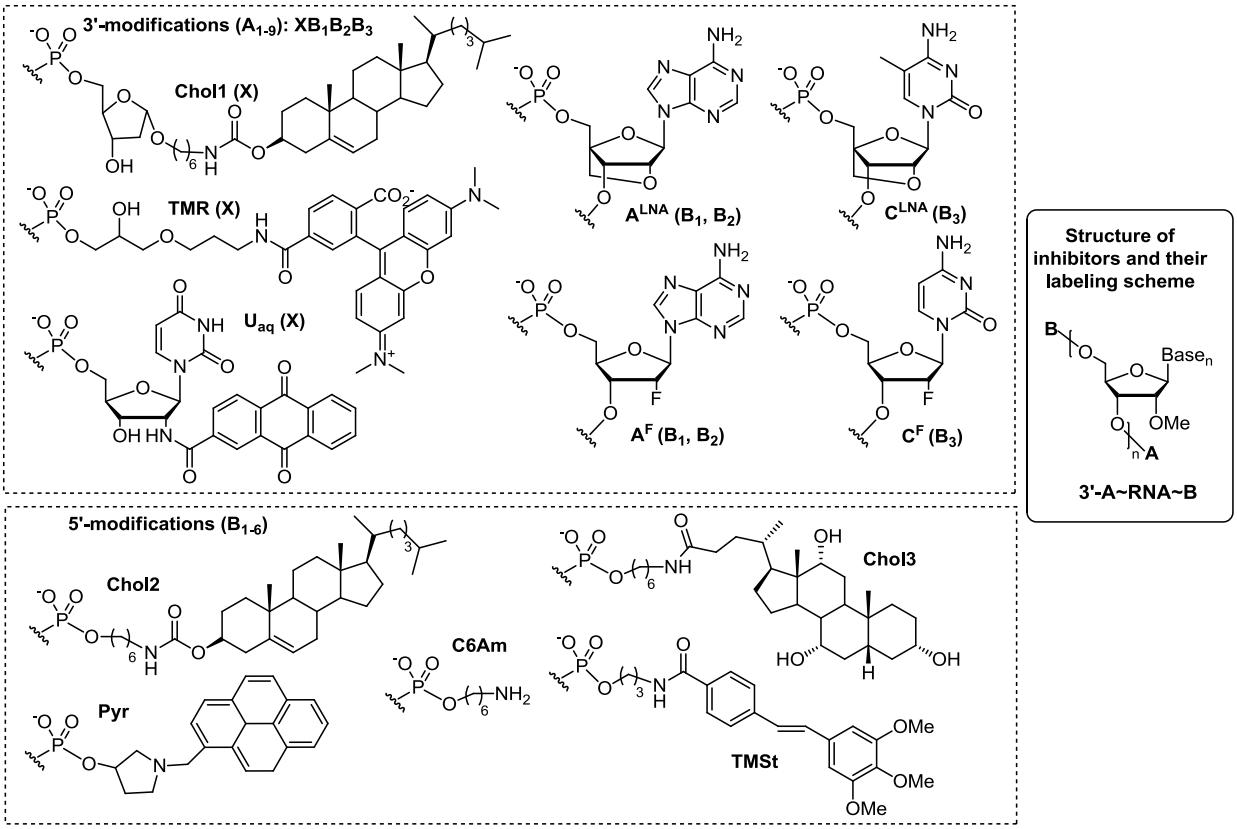

Scheme S1. Structures and labeling scheme of terminal chemical modifications used in this work to optimize antisense activity of 2'-OMe RNA inhibitors of hsa-miR-92 (shortened name miR-92): sequence of the inhibitors (indicated as RNA in the scheme) is 3'-GUGAACAGGGC. For example, according to this labeling scheme fully unmodified, 14-mer inhibitor is A10-RNA-B6.

Table S1. Combinations of 3′ and 5′-terminal modifiers, which were used to modulate properties of 14-mer 2′-OMe RNA inhibitor; 59 new conjugates 3′-A~RNA~B were generated; "H": hydrogen atom

Code	$A_{1\text{-}9}$: 3′-X-$B_1B_2B_3$	Code	$B_{1\text{-}6}$
A1	Chol1-AAC	B1	Chol2
A2	TMR-AAC	B2	Pyr
A3	U_{aq}-AAC	B3	TMSt
A4	H-A^{LNA}AC	B4	C6am
A5	H-$A^{LNA}A^{LNA}$C	B5	Chol3
A6	H-$A^{LNA}A^{LNA}C^{LNA}$	B6	H
A7	H-A^{F}AC		
A8	H-$A^{F}A^{F}$C		
A9	H-$A^{F}A^{F}C^{F}$		
A10	H-AAC		

Synthesis of inhibitors

Inhibitors were synthesized on a H-8 DNA synthesizer on a 1 µmol-scale by using commercially available phosphoramidites and in accordance to the recommendations of the manufacturers. Assembled on the solid phase compounds were cleaved off and deprotected by using concentrated (25 %), aqueous ammonia at 55 °C for 2 h. After removal of ammonia with a N_2-flow, the samples were lyophilized, re-dissolved in water and purified by HPLC by using gradients A-C. Gradient A: in 5 min from 0 to 2 % solution B, in 30 min from 2 to 35 % solution B, in 10 min from 35 to 60 % solution B, in 9 min from 60 to 90 % solution B; gradient B: in 32 min from 0 to 30 % solution B, in 6 min from 30 to 60 %, in 10 min from 60% to 90 %; gradient C: 2 min at 0 % solution B, in 30 min from 0 to 30 % solution B. The new conjugates were identified by MALDI-TOF mass spectrometry and their purity was confirmed by analytical HPLC.

A_1-RNA1-B_1: HPLC gradient A, R_t = 48.2 min; MALDI-TOF MS, negative mode, calculated for $C_{220}H_{216}N_{63}O_{102}P_{15}$ ($[M-H]^-$): *m/z* 6028, found 6024.

A_2-RNA1-B_1: HPLC gradient A, R_t = 44.7 min; MALDI-TOF MS, negative mode, calculated for $C_{216}H_{289}N_{65}O_{106}P_{15}$ ($[M-H]^-$): *m/z* 5942, found 5948.

A_3-RNA1-B_1: HPLC gradient A, R_t = 44.7 min; MALDI-TOF MS, negative mode, calculated for $C_{220}H_{214}N_{63}O_{103}P_{15}$ ($[M-H]^-$): *m/z* 5860, found 5854.

A_4-RNA1-B_1: HPLC gradient B, R_t = 42.4 min; MALDI-TOF MS, negative mode, calculated for $C_{185}H_{254}N_{62}O_{97}P_{14}$ ($[M-H]^-$): *m/z* 5318, found 5318.

A_5-RNA1-B_1: HPLC gradient B, R_t = 42.8 min; MALDI-TOF MS, negative mode, calculated for $C_{185}H_{253}N_{62}O_{97}P_{14}$ ($[M-H]^-$): *m/z* 5316, found 5320.

A_6-RNA1-B_1: HPLC gradient A, R_t = 44.6 min; MALDI-TOF MS, negative mode, calculated for $C_{185}H_{252}N_{62}O_{97}P_{14}$ ($[M-H]^-$): *m/z* 5328, found 5321.

A_7-RNA1-B_1: HPLC gradient A, R_t = 47.3 min; MALDI-TOF MS, negative mode, calculated for $C_{184}FH_{226}N_{62}O_{96}P_{14}$ ($[M-H]^-$): *m/z* 5308, found 5307.

A_8-RNA1-B_1: HPLC gradient B, R_t = 42.9 min; MALDI-TOF MS, negative mode, calculated for $C_{183}F_2H_{225}N_{62}O_{94}P_{14}$ ($[M-H]^-$): *m/z* 5292, found 5293.

A_9-RNA1-B_1: HPLC gradient B, R_t = 42.6 min; MALDI-TOF MS, negative mode, calculated for $C_{182}F_3H_{224}N_{62}O_{94}P_{14}$ ($[M-H]^-$): *m/z* 5284, found 5282.

A_{10}-RNA1-B_1: HPLC gradient A, R_t = 47.3 min; MALDI-TOF MS, negative mode, calculated for $C_{185}H_{255}N_{62}O_{97}P_{14}$ ($[M-H]^-$): *m/z* 5321, found 5319.

A_1-RNA1-B_2: HPLC gradient A, R_t = 48.2 min; MALDI-TOF MS, negative mode, calculated for $C_{207}H_{278}N_{63}O_{102}P_{15}$ ($[M-H]^-$): *m/z* 5785, found 5793.

A_2-RNA1-B_2: HPLC gradient A, R_t = 27.6 min; MALDI-TOF MS, negative mode, calculated for $C_{207}H_{278}N_{63}O_{102}P_{15}$ ($[M-H]^-$): *m/z* 5700, found 5694.

A_3-RNA1-B_2: HPLC gradient A, R_t = 28.7 min; MALDI-TOF MS, negative mode, calculated for $C_{196}H_{235}N_{65}O_{105}P_{15}$ ($[M-H]^-$): *m/z* 5616, found 5627.

A_4-RNA1-B_2: HPLC gradient A, R_t = 26.9 min; MALDI-TOF MS, negative mode, calculated for $C_{172}H_{216}N_{62}O_{95}P_{14}$ ($[M-H]^-$): *m/z* 5076, found 5082.

A_5-RNA1-B_2: HPLC gradient A, R_t = 26.9 min; MALDI-TOF MS, negative mode, calculated for $C_{172}H_{216}N_{62}O_{95}P_{14}$ ($[M-H]^-$): *m/z* 5074, found 5079.

A_6-RNA1-B_2: HPLC gradient A, R_t = 28.5 min; MALDI-TOF MS, negative mode, calculated for $C_{172}H_{214}N_{62}O_{95}P_{14}$ ($[M-H]^-$): *m/z* 5072, found 5082.

A_7-RNA1-B_2: HPLC gradient A, R_t = 27.6 min; MALDI-TOF MS, negative mode, calculated for $C_{171}FH_{214}N_{62}O_{94}P_{14}$ ($[M-H]^-$): *m/z* 5066, found 5077.

A_8-RNA1-B_2: HPLC gradient A, R_t = 27.5 min; MALDI-TOF MS, negative mode, calculated for $C_{170}F_2H_{212}N_{62}O_{93}P_{14}$ ($[M-H]^-$): *m/z* 5054, found 5063.

A_9-RNA1-B_2: HPLC gradient A, R_t = 27.3 min; MALDI-TOF MS, negative mode, calculated for $C_{169}F_3H_{210}N_{62}O_{92}P_{14}$ ($[M-H]^-$): *m/z* 5042, found 5060.

A_{10}-RNA1-B_2: HPLC gradient A, R_t = 26.0 min; MALDI-TOF MS, negative mode, calculated for $C_{169}F_3H_{210}N_{62}O_{92}P_{14}$ ($[M-H]^-$): *m/z* 5078, found 5073.

A_1-RNA1-B_3: HPLC gradient B, R_t = 42.9 min; MALDI-TOF MS, negative mode, calculated for $C_{207}H_{278}N_{63}O_{105}P_{15}$ ($[M-H]^-$): *m/z* 5868, found 5867.

A_2-RNA1-B_3: HPLC gradient A, R_t = 28.7 min; MALDI-TOF MS, negative mode, calculated for $C_{203}H_{255}N_{65}O_{108}P_{15}$ ($[M-H]^-$): *m/z* 5783, found 5749.

A_3-RNA1-B_3: HPLC gradient A, R_t = 31.1 min; MALDI-TOF MS, negative mode, calculated for $C_{196}H_{239}N_{65}O_{109}P_{15}$ ($[M-H]^-$): *m/z* 5700, found 5696.

A_4-RNA1-B_3: HPLC gradient A, R_t = 29.6 min; MALDI-TOF MS, negative mode, calculated for $C_{172}H_{220}N_{62}O_{99}P_{14}$ ($[M-H]^-$): *m/z* 5159, found 5156.

A_5-RNA1-B_3: HPLC gradient B, R_t = 28.6 min; MALDI-TOF MS, negative mode, calculated for $C_{172}H_{119}N_{62}O_{99}P_{14}$ ($[M-H]^-$): *m/z* 5157, found 5157.

A_6-RNA1-B_3: HPLC gradient A, R_t = 31.0 min; MALDI-TOF MS, negative mode, calculated for $C_{172}H_{118}N_{62}O_{99}P_{14}$ ($[M-H]^-$): *m/z* 5169, found 5169.

A_7-RNA1-B_3: HPLC gradient B, R_t = 28.8 min; MALDI-TOF MS, negative mode, calculated for $C_{171}FH_{218}N_{62}O_{98}P_{14}$ ($[M-H]^-$): *m/z* 5149, found 5145.

A_8-RNA1-B_3: HPLC gradient A, R_t = 29.8 min; MALDI-TOF MS, negative mode, calculated for $C_{170}F_2H_{216}N_{62}O_{97}P_{14}$ ($[M-H]^-$): *m/z* 5136, found 5134.

A_9-RNA1-B_3 (labelled as *14-mer*92* in the main text of the paper)*:* HPLC gradient A, R_t = 29.5 min; MALDI-TOF MS, negative mode, calculated for $C_{169}F_3H_{214}N_{62}O_{96}P_{14}$ ($[M-H]^-$): *m/z* 5124, found 5123.

A_{10}-RNA1-B_3: HPLC gradient A, R_t = 28.1 min; MALDI-TOF MS, negative mode, calculated for $C_{172}H_{221}N_{62}O_{99}P_{14}$ ($[M-H]^-$): *m/z* 5161, found 5161.

A_1-RNA1-B_4: HPLC gradient B, R_t = 48.7 min; MALDI-TOF MS, negative mode, calculated for $C_{216}H_{191}N_{63}O_{100}P_{15}$ ($[M-H]^-$): *m/z* 5601, found 5618.

A_2-RNA1-B_4: HPLC gradient B, R_t = 28.2 min; MALDI-TOF MS, negative mode, calculated for $C_{246}H_{187}N_{65}O_{104}P_{15}$ ($[M-H]^-$): *m/z* 5529, found 5527.

A_3-RNA1-B_4: HPLC gradient B, R_t = 26.7 min; MALDI-TOF MS, negative mode, calculated for $C_{181}H_{229}N_{65}O_{105}P_{15}$ ($[M-H]^-$): *m/z* 5446, found 5448.

A_4-RNA1-B_4: HPLC gradient A, R_t = 24.9 min; MALDI-TOF MS, negative mode, calculated for $C_{157}H_{210}N_{62}O_{95}P_{14}$ ($[M-H]^-$): *m/z* 4904, found 4903.

A_5-RNA1-B_4: HPLC gradient A, R_t = 25.9 min; MALDI-TOF MS, negative mode, calculated for $C_{157}H_{209}N_{62}O_{95}P_{14}$ ($[M-H]^-$): *m/z* 4902, found 4900.

A_6-RNA1-B_4: HPLC gradient A, R_t = 24.7 min; MALDI-TOF MS, negative mode, calculated for $C_{157}H_{208}N_{62}O_{95}P_{14}$ ($[M-H]^-$): *m/z* 4914, found 4913.

A_7-RNA1-B_4: HPLC gradient A, R_t = 30.2 min; MALDI-TOF MS, negative mode, calculated for $C_{156}FH_{218}N_{62}O_{94}P_{14}$ ($[M-H]^-$): *m/z* 4894, found 4891.

A_8-RNA1-B_4: HPLC gradient A, R_t = 26.9 min; MALDI-TOF MS, negative mode, calculated for $C_{155}F_2H_{216}N_{62}O_{93}P_{14}$ ($[M-H]^-$): *m/z* 4882, found 4885.

A_9-RNA1-B_4: HPLC gradient A, R_t = 24.5 min; MALDI-TOF MS, negative mode, calculated for $C_{152}H_{214}N_{62}O_{92}P_{14}$ ($[M-H]^-$): *m/z* 4870, found 4869.

A_{10}-RNA1-B_4: HPLC gradient B, R_t = 24.3 min; MALDI-TOF MS, negative mode, calculated for $C_{157}H_{211}N_{62}O_{95}P_{14}$ ($[M-H]^-$): *m/z* 4907, found 4907.

A_1-RNA1-B_5: HPLC gradient A, R_t = 44.9 min; MALDI-TOF MS, negative mode, calculated for $C_{216}H_{312}N_{63}O_{104}P_{15}$ ($[M-H]^-$): *m/z* 5992, found 5998.

A_2-RNA1-B_5: HPLC gradient B, R_t = 33.5 min; MALDI-TOF MS, negative mode, calculated for $C_{212}H_{285}N_{65}O_{108}P_{15}$ ($[M-H]^-$): *m/z* 5919, found 5921.

A_3-RNA1-B_5: HPLC gradient A, R_t = 35.5 min; MALDI-TOF MS, negative mode, calculated for $C_{205}H_{269}O_{109}P_{15}$ ($[M-H]^-$): *m/z* 5837, found 5836.

A_4-RNA1-B_5: HPLC gradient A, R_t = 32.9 min; MALDI-TOF MS, negative mode, calculated for $C_{181}H_{250}N_{62}O_{99}P_{14}$ ($[M-H]^-$): *m/z* 5295, found 5293.

A_5-RNA1-B_5: HPLC gradient A, R_t = 32.5 min; MALDI-TOF MS, negative mode, calculated for $C_{181}H_{249}N_{62}O_{99}P_{14}$ ($[M-H]^-$): *m/z* 5293, found 5294.

A_6-RNA1-B_5: HPLC gradient A, R_t = 33.1 min; MALDI-TOF MS, negative mode, calculated for $C_{181}H_{248}N_{62}O_{99}P_{14}$ ($[M-H]^-$): *m/z* 5305, found 5302.

A_7-RNA1-B_5: HPLC gradient A, R_t = 33.0 min; MALDI-TOF MS, negative mode, calculated for $C_{180}FH_{248}N_{62}O_{98}P_{14}$ ($[M-H]^-$): *m/z* 5285, found 5281.

A_8-RNA1-B_5: HPLC gradient A, R_t = 32.9 min; MALDI-TOF MS, negative mode, calculated for $C_{179}F_2H_{246}N_{62}O_{97}P_{14}$ ($[M-H]^-$): *m/z* 5272, found 5271.

A_9-RNA1-B_5: HPLC gradient A, R_t = 33.2 min; MALDI-TOF MS, negative mode, calculated for $C_{178}F_3H_{244}N_{62}O_{97}P_{14}$ ($[M-H]^-$): *m/z* 5261, found 5259.

A_{10}-RNA1-B_5: HPLC gradient A, R_t = 33.7 min; MALDI-TOF MS, negative mode, calculated for $C_{181}H_{251}N_{62}O_{99}P_{14}$ ($[M-H]^-$): *m/z* 5289, found 5291.

A_1-RNA1-B_6: HPLC gradient A, R_t = 44.7 min; MALDI-TOF MS, negative mode, calculated for $C_{185}H_{255}N_{62}O_{97}P_{14}$ ($[M-H]^-$): *m/z* 5435, found 5435.

A_2-RNA1-B_6: HPLC gradient A, R_t = 27.3 min; MALDI-TOF MS, negative mode, calculated for $C_{181}H_{228}N_{64}O_{101}P_{14}$ ($[M-H]^-$): *m/z* 5350, found 5353.

A_3-RNA1-B_6: HPLC gradient A, R_t = 27.3 min; MALDI-TOF MS, negative mode, calculated for $C_{174}H_{212}N_{64}O_{102}P_{14}$ ($[M-H]^-$): *m/z* 5268, found 5265.

A_4-RNA1-B_6: HPLC gradient A, R_t = 24.9 min; MALDI-TOF MS, negative mode, calculated for $C_{150}H_{194}N_{61}O_{92}P_{13}$ ($[M-H]^-$): *m/z* 4725, found 4726.

A_5-RNA1-B_6: HPLC gradient B, R_t = 24.1 min; MALDI-TOF MS, negative mode, calculated for $C_{150}H_{192}N_{61}O_{92}P_{143}$ ($[M-H]^-$): *m/z* 4723, found 4724.

A_6-RNA1-B_6: HPLC gradient A, R_t = 24.0 min; MALDI-TOF MS, negative mode, calculated for $C_{150}H_{191}N_{61}O_{92}P_{13}$ ($[M-H]^-$): *m/z* 4735, found 4737.

A_7-RNA1-B_6: HPLC gradient A, R_t = 27.6 min; MALDI-TOF MS, negative mode, calculated for $C_{149}H_{191}N_{61}O_{91}P_{13}$ ($[M-H]^-$): *m/z* 4715, found 4713.

A_8-RNA1-B_6: HPLC gradient A, R_t = 25.1 min; MALDI-TOF MS, negative mode, calculated for $C_{148}F_2H_{189}N_{61}O_{90}P_{13}$ ($[M-H]^-$): *m/z* 4703, found 4700.

A_9-RNA1-B_6: HPLC gradient A, R_t = 25.1 min; MALDI-TOF MS, negative mode, calculated for $C_{147}F_3H_{187}N_{61}O_{89}P_{13}$ ($[M-H]^-$): *m/z* 4691, found 4692.

A_{10}-RNA1-B_6 (labelled as *14-mer92* in the main text of the paper)*:* HPLC gradient A, R_t = 25.2 min; MALDI-TOF MS, negative mode, calculated for $C_{150}H_{194}N_{61}O_{92}P_{13}$ ($[M-H]^-$): *m/z* 4728, found 4729.

*14-mer*30b:* HPLC gradient C, R_t = 23.4 min; MALDI-TOF MS, negative mode, calculated for $C_{146}H_{192}N_{50}O_{96}P_{13}$ ($[M-H]^-$): *m/z* 4586, found 4585.

*14-mer*92_a:* HPLC gradient B, R_t = 29.1 min; MALDI-TOF MS, negative mode, calculated for $C_{168}H_{213}N_{59}O_{97}P_{14}$ ($[M-H]^-$): *m/z* 5085, found 5086.

*14-mer*92_b:* HPLC gradient B, R_t = 29.1 min; MALDI-TOF MS, negative mode, calculated for $C_{168}H_{213}N_{59}O_{97}P_{14}$ ($[M-H]^-$): *m/z* 5085, found 5080.

*14-mer*92_c:* HPLC gradient B, R_t = 29.2 min; MALDI-TOF MS, negative mode, calculated for $C_{168}H_{213}N_{59}O_{97}P_{14}$ ($[M-H]^-$): *m/z* 5085, found 5089.

21-mer92: HPLC gradient C, R_t = 21.7 min; MALDI-TOF MS, negative mode, calculated for $C_{224}H_{292}N_{89}O_{140}P_{20}$ ($[M-H]^-$): *m/z* 3690, found 3690.

21-mer92_a: HPLC gradient B, R_t = 26.7 min; MALDI-TOF MS, negative mode, calculated for $C_{223}H_{291}N_{86}O_{141}P_{20}$ ($[M-H]^-$): *m/z* 7052, found 7047.

21-mer92_b: HPLC gradient B, R_t = 25.5 min; MALDI-TOF MS, negative mode, calculated for $C_{223}H_{291}N_{86}O_{141}P_{20}$ ($[M-H]^-$): *m/z* 7052, found 7048.

21-mer92_c: HPLC gradient B, R_t = 25.3 min; MALDI-TOF MS, negative mode, calculated for $C_{223}H_{291}N_{86}O_{141}P_{20}$ ($[M-H]^-$): *m/z* 7052, found 7049.

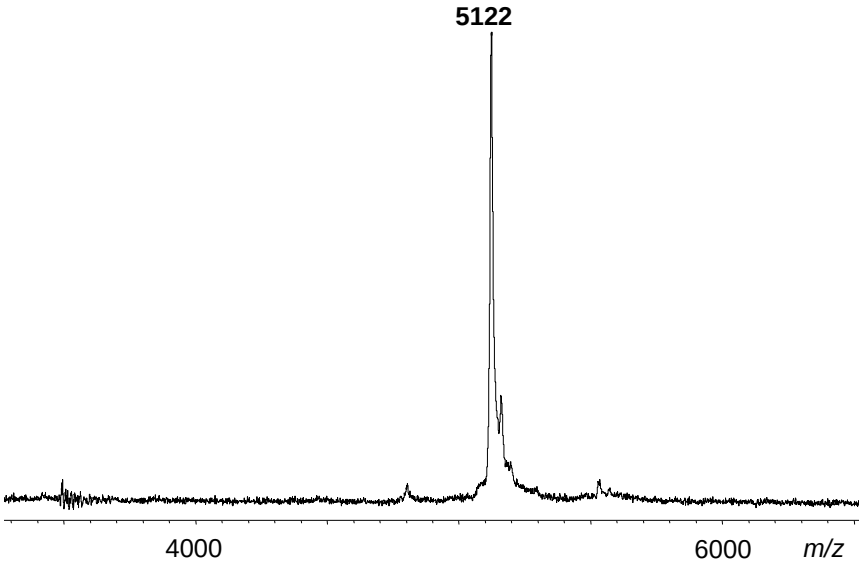

Figure **S1**. MALDI-TOF mass spectrum of a representative inhibitor (14-mer*92).

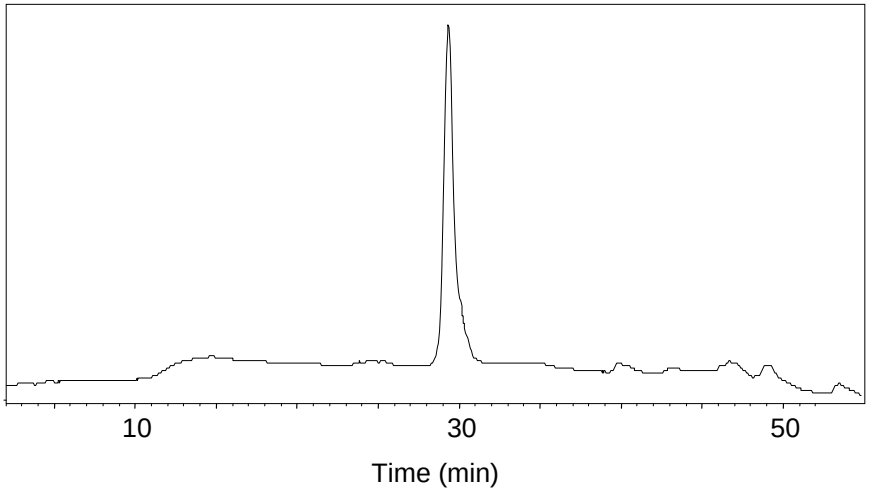

Figure **S2**. HPLC profile of a representative inhibitor (14-mer*92).

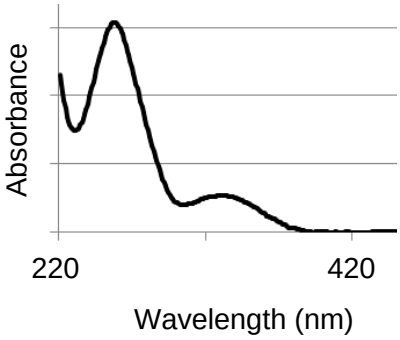

Figure **S3**. UV-visible spectrum of a representative inhibitor (14-mer*92).

To estimate the affinity of the inhibitors to miR-92l, inhibitor / miR-92l duplexes were assembled in the presence of SYBR® Green I (Life Technologies). This dye is practically not fluorescent in aqueous solution, whereas in the presence of nucleic acid duplexes its highly fluorescent, intercalated form is formed.[1] Correspondingly, temperature (t) dependent duplex dissociation and association cause changes of the fluorescent intensity characteristic for SYBR® Green I that allows determining melting points of the duplexes (T_m). T_m's of the duplexes were determined as maxima in plots of -dF/dt vs t. It has been reported that T_m's obtained by this method correlate with the values obtained by using UV-visible spectroscopy.[2] We selected the former approach, since it requires substantially lower amounts of conjugates. For selected conjugates we also determined T_m's by the conventional method using UV-visible spectroscopy. UV-T_m's apparently correlate with fluorescence-T_m's, however, the correlation curve is rather noisy (Figure S4). Therefore, fluorescence-T_m values were applied only as a rough estimate of affinity of the inhibitors to their targets in the initial inhibitor screen (Table S2), whereas UV- T_m's were applied to evaluate the affinity to RNA targets of most active inhibitors discussed in the main part of the paper.

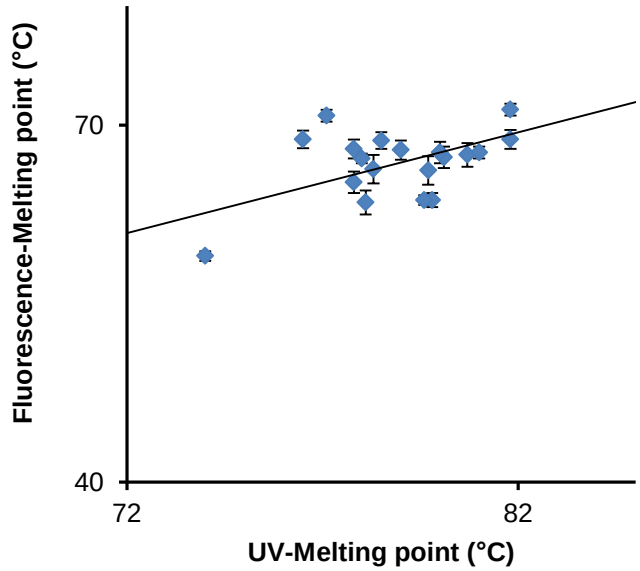

Figure S4. Correlation between melting points of selected inhibitor/miR-92l duplexes measured by using either UV-visible spectrophotometer (UV-Melting point) or RT PCR instrument in combination with a duplex-specific dye Sybr Green I (Fluorescence-Melting point); conditions for measurements of UV-T_m: phosphate-buffered (pH 7, 10 mM) saline (150 mM), duplex concentration 1 µM; conditions for measurements of fluorescence-T_m: phosphate-buffered saline, pH 7, 10 mM, duplex concentration 10 µM.

Table S2. Efficiency of inhibition of miR-92 in HeLa cells (activity) by A~RNA~B as well as positive (21-mer) and negative (anti-bantam[i]) controls, and melting points (fluorescence-T_m) of duplexes of the 14-mers and miR-92as.[ii]

A-RNA-B	*Activity / T_m (°C)*	*A-RNA-B*	*Activity / T_m (°C)*	*A-RNA-B*	*Activity / T_m (°C)*
A1B1	1.4 ± 0.4 / -	A1B2	6.1 ± 2.5 / -	A1B3	7.9 ± 2.6 / 63.4 ± 0.3
A2B1	2.4 ± 0.7 / -	A2B2	2.0 ± 0.6 / -	A2B3	1.8 ± 0.2 / -
A3B1	3.3 ± 1.6 / -	A3B2	7.0 ± 1.4 / 63.5 ± 1.0	A3B3	- / 68.0 ± 0.8
A4B1	1.7 ± 0.9 / -	A4B2	6.7 ± 1.6 / 65.2 ± 0.9	A4B3	3.8 ± 0.9 / 67.9 ± 0.8
A5B1	1.3 ± 0.5 / -	A5B2	2.5 ± 0.4 / 67.3 ± 0.9	A5B3	3.1 ± 2.0 / 71.7 ± 0.6
A6B1	1.8 ± 0.3 / 58.0±0.4	A6B2	3.7 ± 1.6 / 68.8 ± 0.8	A6B3	3.2 ± 1.3 / 71.3 ± 0.5
A7B1	1.7 ± 0.4 / -	A7B2	5.0 ± 1.6 / 67.2 ± 0.4	A7B3	7.7 ± 2.8 / 67.6 ± 0.7
A8B1	1.5 ± 0.5 / -	A8B2	5.4 ± 2.6 / 63.7 ± 0.6	A8B3	5.7 ± 2.2 / 63.7 ± 0.4
A9B1	1.6 ± 1.1 / 55.4±0.2	A9B2	5.8 ± 4.1 / 68.7 ± 0.7	A9B3	8.7 ± 3.2 / 70.8 ± 0.5
A10B1	1.4 ± 0.3 / 59.0±0.4	A10B2	2.2 ± 0.1 / -	A10B3	4.3 ± 0.9 / 69.9 ± 0.9

A-RNA-B	*Activity / T_m (°C)*	*A-RNA-B*	*Activity / T_m (°C)*	*A-RNA-B*	*Activity / T_m (°C)*
A1B4	7.5 ± 2.2 / -	A1B5	7.7 ± 6.4 / 63.0 ± 0.3	A1B6	6.1 ± 1.9 / -
A2B4	6.7 ± 1.9 / -	A2B5	4.2 ± 1.6 / -	A2B6	1.8 ± 0.9 / -
A3B4	10.2 ±3.4/ 73.5±0.4	A3B5	10.7 ± 3.9 / 65.4 ±1.1	A3B6	6.9 ± 2.4 / 66.3 ± 1.2
A4B4	6.9 ± 3.9/ 66.2± 1.2	A4B5	5.2 ± 1.6 / 66.5 ± 0.9	A4B6	2.9 ± 0.9 / 67.7 ± 0.5
A5B4	6.1 ± 2.3 / -	A5B5	4.1 ± 2.0 / 69.8 ± 0.9	A5B6	2.2 ± 0.9 / 72.1 ± 0.6
A6B4	5.9 ± 1.8 / 75.1±0.2	A6B5	6.1 ± 2.4 / 72.7 ± 0.8	A6B6	2.8 ± 1.1 / 72.0 ± 0.5
A7B4	3.3 ± 0.8 / 69.2±0.5	A7B5	5.0 ± 2.6 / 64.7 ± 1.0	A7B6	4.1 ± 0.8 / 71.7 ± 1.0
A8B4	3.9 ± 1.1 / 67.7±0.9	A8B5	7.2 ± 3.1 / 69.9 ± 0.8	A8B6	2.4 ± 0.6 / 72.6 ± 0.9
A9B4	2.0 ± 0.9 / 73.1±0.8	A9B5	5.7 ± 2.2 / 68.3 ± 0.6	A9B6	2.3 ± 1.2 / 73.8 ± 0.7
A10B4	5.7 ± 1.8 / 67.5±1.0	A10B5	6.8 ± 3.0 / 64.8 ± 1.2	A10B6	2.6 ± 1.9 / 68.6 ± 0.3

[i] Bantam is drosophila miRNA. Since it has no homologs in human, it can serve as a negative control for the experiments in human cells

[ii] Activity / T_m parameters for the positive control (21-mer92) were found to be 7.3 ± 2.6 / 77.0 ± 0.4 °C, for the truncated strand (A_{10}-RNA-B_6 or 14-mer92) - 2.6 ± 1.9 / 68.6 ± 0.3 °C and for the negative control (anti-bantam) - 1.1 ± 0.3 / no melting profile was observed; inhibitors, which increase expression of hRluc by more than 5.7 fold, are indicated with red color.

All prepared conjugates, which contain 5′-cholesteryl fragment (B1), exhibited practically no inhibition of miR-92 in cells (Table S2). T_m's of duplexes of miR-92l with three representatives of this series could be determined (A_6-RNA-B_1, A_9-RNA-B_1, A_{10}-RNA-B_1), whereas other duplexes were found to melt irreversibly. The T_m's obtained were 9.4 – 14.6 °C lower than the T_m of the unmodified 14-mer/miR-92l duplex. Therefore, we could conclude that the low activity of the B_1-containing inhibitors is caused by their low affinity towards miR-92l. In contrast, the conjugates with no 5′-modification ($A_{1\text{-}6}$~RNA-B_6) were found to bind miR-92as with rather high affinity as it is indicated by the melting points of the corresponding duplexes (T_m's= 66.3 - 73.8 °C). However, the antisense activity of 8 out of 10 conjugates of this series was lower or equal to that of the unmodified 14-mer (Table S2). Conjugate A_3~RNA1-B_6, whose duplex with miR-92l melts at the lowest in this series temperature (66.3 ± 1.2 °C), and

conjugate A_1~RNA1-B_6, whose duplex with miR-92l melts irreversibly, were found to be 2.3-2.7 fold more active than the unmodified 14-mer. These data indicate that there is no simple correlation of the biological activity with the affinity of the inhibitors to their targets.

Analysis of the activity data for 59 chemically modified inhibitors and 3 controls presented in Table S2 and its footnotes reveal that the most favorable 3′-modifications are the 3′-cholesterol containing residue A_1 and the 5′-anthraquinone fragment A_3, whereas LNA (A_{4-6}) and F-RNA (A_{7-9}) residues are less efficient. Most favorable 5′-modifications were found to be the aminohexyl B_4 and the cholic acid residue B_5 and slightly less efficient – pyrene residue B_2 and trimethoxystilbene residue B_3. We observed that the best combinations of the 5′- and 3′-modifiers attached to the 14-mer 2′-OMe RNA sequence (shown with red color in Table S2) lead to inhibitors, which exhibit 80-150 % of the efficiency of the 21-mer92, whereas the unmodified 14-mer92 exhibits only ca. one third (36 %) of the activity of the 21-mer92. Thus, we demonstrated that by introduction of chemical modifications at the 3′- and 5′-termini of short 2′-OMe RNAs one can convert them to efficient inhibitors of micro RNAs.

We were surprised to observe that the most active inhibitors were not those ones having the highest affinity towards the complementary RNA. For example, three most active inhibitors were found to be A_9~RNA-B_3, A_3~RNA-B_4, A_3~RNA-B_5 (Table S2). T_m's of the duplexes of miR-92l with these conjugates are 70.8 $\pm$ 0.5, 73.5 $\pm$ 0.4 and 65.4 $\pm$ 1.1 °C correspondingly. In contrast, the duplex A_9~RNA-B_4/miR-92l melts at 73.1 $\pm$ 0.8 °C, whereas this conjugate was found to be practically inactive. The data presented in Table S2 allow us concluding that inhibitors, which form inhibitor/miR-92l duplexes with T_m's > 60 °C, can exhibit biological activity, whereas those having lower affinity towards miR-92l are inactive.

For further optimizations of the inhibitors of miR-92 we selected the combination of modifiers 3′-A_9 and 5′-B_3, since handling of the conjugates containing the anthraquinone residue A_3 was found to be difficult. In particular, their stock solutions were not stable for long time and their HPLC purification was complicated by the strong absorption of the conjugates on the HPLC column. These properties can be explained by the hydrophobic character of the A_3-containing conjugates.

Determination of melting points (T_m's)

UV melting experiments were performed on a Varian Cary 100 Bio UV-vis spectrophotometer measuring absorbance at 260 nm in 1 cm black wall semimicrocuvettes with sample volume of 0.7 mL, 1 μM strand concentration in DBPS buffer (pH 7, 150 mM). Cooling and heating rates were 0.5 ^{o}C/min. Melting points were averages of the extrema of the first derivative of the 61-point smoothed curves from at least 2 cooling and 2 heating curves. Representative melting profiles and their first derivative are shown in Figure S5.

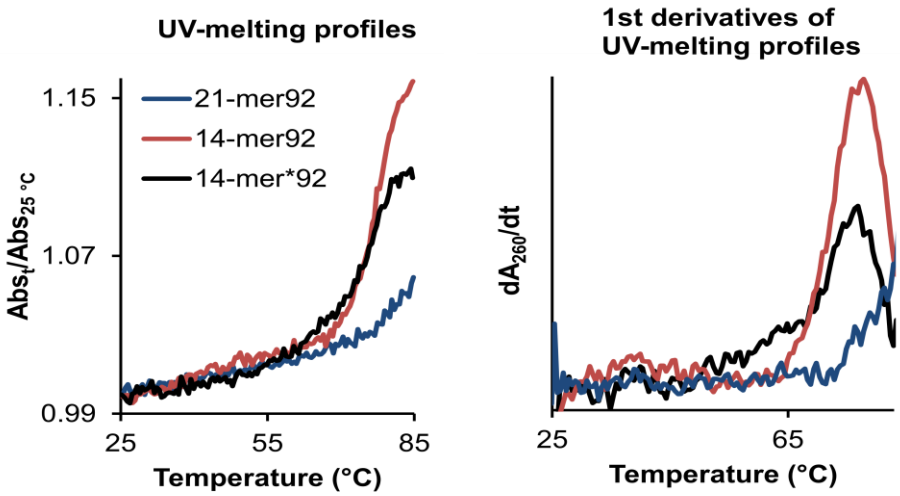

Figure S5. UV-melting profiles and their first derivatives measured for solutions containing duplexes, which consist of miR-92l (1 μM) and 1 eq of an inhibitor indicated on the plot. Absorbance at 260 nm was measured as a function of temperature; ratio of absorbance at a particular temperature (A_t) and absorbance at 25 °C ($A_{25\ °C}$) is plotted on the OY axis) Other experimental conditions are provided in the text above.

SYBR® Green I (2-{2-[(3-dimethylaminopropyl)-propylami-no]-1-phenyl-1*H*-chinolin-4-ylidenmethyl)-3-methylbenzothia-zol-3-ium-cation) is a weakly fluorescent dye. However, when bound to the double stranded nucleic acid structure, it fluoresces strongly. We applied this compound as an indicator of duplex formation and dissociation for determination of melting points (T_m's) of inhibitor/target associates. In particular, T_m's were determined as maxima of the first derivative of the temperature dependence of the fluorescence at λ_{em}= 530 nm (λ_{ex}= 470 nm) of inhibitor (10 μM), target (10 μM) and SYBR® Green I (Life Technologies, 1:40000 diluted) mixtures in phosphate buffer (10 mM, pH 7, total volume is 20 μL): $T_m = -(dF/dt)_{max}$. The data are presented in Tables S2 and S3.

Table S3. Fluorescence-melting points of duplexes of miR-92l with fully matched 21-mer92 and 14-mer*92 inhibitors and their mismatched analogues

Inhibitor (5'→3')	T_m (°C)	ΔT_m (°C)
21-mer92: CAGGCCGGGACAAGUGCAAUA	77.0 ± 0.4	0
21-mer92_a: CAGGCC**U**GGACAAGUGCAAUA	69.6 ± 0.7	-7.4
21-mer92_b: CAGGCCG**U**GACAAGUGCAAUA	66.0 ± 0.6	-11.0
21-mer92_c: CAGGCCGG**U**ACAAGUGCAAUA	69.9 ± 0.6	-7.1
14-mer92: *B3* CGGGACAAGUG *A9*[l]	68.6 ± 0.5	0
14-mer92_a: *B3* C**U**GGACAAGUG *A9*	59.7 ± 0.5	-8.9
14-mer92_b: *B3* CG**U**GACAAGUG *A9*	52.3 ± 0.5	-16.3
14-mer92_c: *B3* CGG**U**ACAAGUG *A9*	50.9 ± 0.6	-17.7

[l] see structures of modifiers B3 and A9 in Scheme S1.

Cellular assays. *Cells and cell culture*. The human cervical cancer cells line (HeLa TK) was cultured in Eagle's minimum essential medium (EMEM) supplemented with 10% fetal calf serum (FCS), 1% L-glutamine, and 1% penicillin/streptomycin. 24 h before the transfection the cells were detached from the surface by using trypsin (0.05%)/ethylenediamine tetracetic acid (EDTA, 0.02 %) solution, washed with Dulbecco's phosphate-buffered saline (DPBS), re-suspended in the fresh medium and diluted with the medium to 150 cells/µL. Next, aliquots (100 µL) of such suspensions were placed into wells of 96-well microtiter plates and the cells were allowed to get attached to the surface for 24 h in the incubator at 37 °C, 95 % air humidity and 5 % CO_2 content.

Plasmids

Luciferase reporter plasmids (psiCHECK-2-miR-92 and psiCHECK-2-miR-30b) were used to measure the intracellular activity of hsa-miR-92 and hsa-miR-30b. They were generated by cloning corresponding double-stranded DNA fragments that contain single complementary miR-92 or miR-30bbinding sites into XhoI- and NotI-digested psiCHECK™-2 vector (Promega) immediately downstream of *Renilla* luciferase (hRluc) gene. Blue-script II KS (+/-) plasmid (Stratagene) was used as functionally neutral vector to reach the recommended plasmid concentration using Lipofectamine™ 2000 (Invitrogen) as transfection reagent.

Tranfection and monitoring of miR-activity monitoring by using the dual luciferase assay. Determination of IC_{50}-values for miR-92 inhibitors

First, a mixture of Bluescript II KS (+/-) plasmid (10 ng, 4.9 µL), either psiCHECK-2-miR-92 or psiCHECK-2-miR-30b plasmid (10 ng, 2.6 µL) and a corresponding inhibitor (5 pmol, 2.5 µL; for IC_{50} measurements: 0.1 – 10 pmoles) was prepared in the reduced serum medium (Opti-MEM, 25 µL). Then, Lipofectamine™ 2000 (0.4 µL) was mixed with Opti-MEM (24.6 µL) and incubated for 5 min at 22°C. The resulting solution was added to plasmid/inhibitor mixtures and incubated for another 20 min at 22°C. The medium of the cells was replaced with Dulbecco's modified Eagle's medium (DMEM) containing 1% glutamine and the transfection mixtures (50 µL). After 4 h incubation at 37°C, 95 % air humidity and 5 % CO_2, the medium was replaced with DMEM supplemented with 10% fetal calf serum (FCS), 100 U/mL penicillin, 100 µg/mL streptomycin, 2 mM L-glutamine. After another 20 h of incubation at the same conditions, the medium was removed and cells were washed with DPBS buffer. For the measurement of Fluc and hRluc activities, the Dual-Luciferase® Reporter Assay kit (Promega) was applied. Cells were lysed with the passive lysis buffer (50 µL, Promega) and shaked for 15 min. For the measurement of luciferase activities, cell lysate (10 µL) was diluted with the passive lysis buffer (90 µL) and the resulting mixture was transferred to the white 96-well microplate. Then, luciferase assay reagent II (LARII, 25 µL) was added to this mixture. After shaking for 2 s, the chemiluminescence signal was acquired for 12 s. The intensity of this signal correlates with the activity of Fluc. Next, Stop&Glo® reagent was injected (25 µL), the mixture was shaked for 2 s and the chemiluminescence signal was acquired for 6 s. The intensity of this signal correlates with the activity of hRluc. In order to determine hsa-miR-92a and hsa-miR-30b activity, the chemiluminescence intensity of hRluc was normalized to the intensity of Fluc encoded in psiCHECK-2-miR-92 or psiCHECK-2-miR-30b plasmids and used as internal control for the transfection efficiency.

Assaying stability of inhibitors in cell lysates

The human cervical cancer cells line (HeLa TK) was cultured in Eagle's minimum essential medium (EMEM) supplemented with 10% fetal calf serum (FCS), 1% L-glutamine, and 1% penicillin/streptomycin. 24 h before the experiment the cells were detached from the surface by using trypsin (0.05 %)/ethylenediamine tatracetic acid

(EDTA, 0.02 %) solution, washed with Dulbecco's phosphate-buffered saline (DPBS), re-suspended in the fresh medium and diluted up with the medium to 150 cells/µL. Next, portions (100 µL) of such suspensions were placed into wells of 96-well microtiter plates and the cells were allowed to get attached to the surface for 24 h in the incubator at 37 °C, 95 % air humidity and 5 % CO_2 content. Then the cells were lysed with the passive lysis buffer (50 µL, Promega), which is not denaturing proteins, and shaked for 15 min. Inhibitors (100 pmoles per well, 21-mer92, 14-mer92 and 14-mer*92 were tested) were added and allowed to incubate for up to 229 min. The probes (10 µL) were taken during the incubation and analyzed by HPLC. We observed that three studied inhibitors were stable at these conditions. Representative HPLC traces are shown in Figure S6.

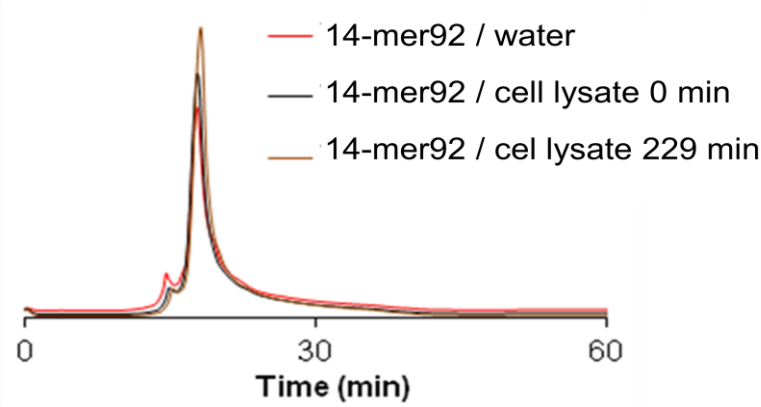

Figure S6. HPLC-profiles of a representative 2'-OMe RNA inhibitor (14-mer), which was incubated in cellular lysate for 0 (black trace) and 229 min (brown trace); for comparison an HPLC profile of the pure inhibitor dissolved in water is also provided (red trace); the data indicate that no significant degradation of 2'-OMe RNA is observed at these experimental conditions

References

1. https://www.lifetechnologies.com/de/de/home.html.

2. (a) Gudnason, H.; Dufva, M.; Bang, D. D.; Wolff, A. *Nucleic Acids Res.* 2007, *35*, e127. (b) Kenski, D. M.; Cooper, A. J.; Li, J. J.; Willingham, A. T.; Haringsma, H. J.; Young, T. A.; Kuklin, N. A.; Jones, J. J.; Cancilla, M. T.; McMasters, D. R.; Mathur, M.; Sachs, A. B.; Flanagan, W. M. *Nucleic Acids Res.* 2010, *38*, 660.